

IN 35

171961

PII

NASA Technical Memorandum 106219

Acousto-Ultrasonic Analysis of Failure in Ceramic Matrix Composite Tensile Specimens

Harold E. Kautz
Lewis Research Center
Cleveland, Ohio

and

Abhisak Chulya
Cleveland State University
Cleveland, Ohio

Prepared for the
Second International Conference on Acousto-Ultrasonics
sponsored by the American Society for Nondestructive Testing, Inc.
Atlanta, Georgia, June 24-25, 1993



(NASA-TM-106219)
ACOUSTO-ULTRASONIC ANALYSIS OF
FAILURE IN CERAMIC MATRIX COMPOSITE
TENSILE SPECIMENS (NASA) 10 p

N93-29073

Unclass

G3/38 0171961



ACOUSTO-ULTRASONIC ANALYSIS OF FAILURE IN CERAMIC MATRIX
COMPOSITE TENSILE SPECIMENS

Harold E. Kautz
National Aeronautics and Space Administration
Lewis Research Center
Cleveland, Ohio 44135
(216) 433-6015

and

Abhisak Chulya
Cleveland State University
Cleveland, Ohio 44115

ABSTRACT

Three types of acousto-ultrasonic (AU) measurements: stress-wave factor (SWF), lowest antisymmetric plate mode group velocity (VS), and lowest symmetric plate mode group velocity (VL), were performed on specimens before and after tensile failure. Three different Nicalon fiber architectures with ceramic matrices were tested. These composites were categorized as 1D (unidirectional fiber orientation) SiC/CAS glass ceramic, and 2D and 3D woven SiC/SiC ceramic matrix materials. SWF was found to be degraded after tensile failure in all three material categories. VS was found to be degraded only in the 1D SiC/CAS. VL was difficult to determine on the irregular specimen surfaces but appeared unchanged on all failed specimens. 3D woven specimens with heat-treatment at high temperature exhibited degradation only in SWF.

INTRODUCTION

The acousto-ultrasonic (AU) approach to nondestructive characterization has been shown to be useful in assessing mechanical properties in composite structures [1-7]. This has been achieved by comparing AU results with models for the propagation of ultrasound in composites as they relate to the material/mechanical state of the specimen. The understanding gained by this comparison has led to useful NDE tools for evaluating ceramic matrix composite (CMC) structures.

In early work [2] the stress-wave factor, SWF, calculated from AU signals, was used to assess the mechanical state of a specimen. In general, SWF a function of the magnitude of the AU signal recovered at the receiver. SWF can also be the time decay of the signal. In the form of a ring-down count, this decay concept was originally borrowed from acoustic emission. Recently, conditions have been explored where diffuse decay rate measurements can be used as a more detailed substitute for ring-down.

More recently, [1,8,9], plate wave analysis has been shown useful for characterizing composites in terms of the various stiffness moduli.

This work examines both SWF and plate wave analysis of data acquired with the AU configuration. The objective is to assess its practicality for monitoring changes due to mechanical degradation in CMCs with various fiber architectures. The acousto-ultrasonic configuration is applied to collect data on CMC tensile specimens of three different fiber layouts.

MATERIALS DESCRIPTION

The three ceramic matrix composite (CMC) systems investigated were unidirectional reinforced (1D) SiC fiber/calcium aluminosilicate (CAS), 2D plain weave SiC fiber/SiC, and 3D woven SiC fiber/SiC overcoated composites. SiC/CAS CMC was fabricated by Corning Inc. and SiC/SiC systems were infiltrated by DuPont Co. Nicalon SiC fibers with 40 percent volume were used in all three systems. Tensile tests were performed at room temperature for 1D SiC/CAS and 2D SiC/SiC while 3D SiC/SiC tensile specimens were tested at 1200 and 1400 °C for short term exposure in air. Two 3D SiC/SiC specimens were also heat-treated at 1200 and 1550 °C for 100 hr in air and then tensile-tested at room temperature. A detailed description of 3D fiber architecture and composite fabrication is reported elsewhere [10].

BASIS OF EXPERIMENT

Lowest mode plate wave velocities respond to changes in stiffness and flexure moduli [8,9,11]. SWF will respond to changes in attenuation. A source of attenuation is the formation of matrix cracks in the failed specimens. These cracks may act as reflecting discontinuities. The increase in attenuation is not due to transformation of ultrasonic energy to another form, but rather a result of scatter out of the beam.

Plate wave velocity and SWF are global variables. One looks for an average value for the entire gauge region. In the tensile failed specimen one may expect the mechanical/material properties to vary as a function of position along the gauge length. In the case of plate waves, nonlinearity of the plot of transducer separation versus pulse arrival time may reflect variation in velocity, and hence modulus, along the gauge region between the grip and the fracture surface.

In the case of SWF, diffuse field decay analysis has been shown applicable to tensile specimens [12-14]. However, diffuse field decay may be too global to reflect variations in attenuation along the gauge. Thus, the method of moments [15,16] is applied to AU signals collected over sets of relatively narrow transducer separations along the gauge. The stress-wave factor is defined as the centroid of the power spectrum, $P(f)$:

$$SWF = \left[\frac{\int_{f_1}^{f_2} P(f) \cdot f \cdot df}{\int_{f_1}^{f_2} P(f) \cdot df} \right] \quad (1)$$

In Eq. (1), the variable f is frequency. In the present work we take the limit f_1 as zero and f_2 is the Nyquist frequency for the digitized time domain AU signal. The SWF defined in Eq. (1) is sensitive to changes in shape of the spectrum such as might be produced by changes in attenuation. At the same time, it is normalized to minimize scatter due to surface coupling effects.

EXPERIMENTAL PROCEDURE

Acousto-ultrasonic data collection and processing have been described earlier [1,4,9]. Figure 1 shows the AU configuration on a tensile specimen for plate wave excitation and conventional stress-wave factor determination. Plate waves were excited and received with pairs of 0.5 or 1.0 MHz transducers. SWF was determined using pairs of 2.25 MHz transducers. In all cases broad-band immersion transducers were used with elastic coupling pads.

Measurements were performed on undamaged and failed specimens. The effect of tensile stress to failure on these three types of CMCs is examined by comparing AU parameters of the undamaged to that of the failed specimen for each fiber architecture. All specimens had tensile grip reinforcements attached before AU

measurement. For plate waves, it was found practical to couple the sending transducer to a grip while the receiver was moved over a range of positions on the gauge region. This is illustrated in Fig. 2. The slope of the transducer separation, s , versus pulse arrival time gives the mode velocity. Departure of this plot from linearity in a failed specimen may be interpreted as a response of the particular plate mode to strain induced degradation. For the plate wave measurements the total force on the two couplant pads was 2.5 N.

For SWF measurements, both transducers were coupled to the gauge region. For these measurements the transducer centerline separation, s , was constant at 1.908 cm. The total force on the two coupling pads was 12 N.

RESULTS AND DISCUSSION

Centroid of the Power Spectrum as Stress-Wave Factor

Figure 3 shows SWF data for the 3D woven, nonheat treated, specimens tested at elevated temperature. The centroid of the power spectrum, defined in Eq. (1), is plotted against the center line of the receiving transducer position where the wave form was collected. The open squares indicate \pm one standard deviation of values on the untested specimen. They were taken at positions along the gauge region from one end to the other. The filled squares show standard deviations for data on the failed specimen. These were taken at positions starting next to one grip and continuing up to the break. This SWF shows no gradient along the gauge region in the failed specimens. Thus no gradient in matrix crack density can be identified in the failed 3D ceramic composite.

Average SWF for 1D SiC/CAS, 2D SiC/SiC, and 3D SiC/SiC failed at elevated temperatures are compared in Fig. 4. In all three cases the centroid of the power spectrum is degraded to a lower frequency after failure. This is taken as an increase in attenuation due to matrix crack formation. The degradation is most pronounced in the 1D SiC/CAS.

It is evident that SWF before and after tensile tests should be compared only within the same composite system. For example, the highest SWF values before tensile test were found in the 1D SiC/CAS. However this does not relate to ability to withstand strain. The 2D and 3D architectures possess fibers across the ultrasound path which produce the greater initial attenuation.

Shear Velocity From the First Antisymmetric Plate Mode

Figures 5 to 7 exhibit representative sets of lowest antisymmetric plate mode pulse arrival times for the 1D SiC/CAS, 2D SiC/SiC, and 3D SiC/SiC failed at elevated temperature respectively. Slopes on these plots are a measure of velocity. Significant variation in slope from point to point might be taken as indicating variation of shear stiffness along the gauge. The small variations observed here are probably scatter in the data, revealing no stiffness gradient.

Linear regression was performed on these data in order to obtain an average shear velocity for the gauge region. Figure 8 compares undamaged and failed specimen velocities for the three fiber architectures. This plot shows a one standard deviation range for each set. Although the \pm one standard deviation intervals overlap before and after for each system, the 1D SiC/CAS shows greatest probability of decreased shear velocity, and hence shear stiffness degradation after failure.

Longitudinal Velocity From the First Symmetric Plate Mode

Figures 9 to 11 exhibit representative sets of lowest symmetric plate mode pulse arrival times for the same composite specimens of the previous section. These data show much more scatter than the antisymmetric pulse data of Figs. 5 to 7. This was caused by the very nonplanar surfaces. One expects that surface nonsmoothness of

this kind will tend to inhibit formation of plate wave pulses. Symmetric pulses are generally less robust than the antisymmetric. In the present study the symmetric pulses were often difficult to window, thus leading to scatter in transit time.

Figure 12 shows the regression slope velocity data for all three systems. The 1D SiC/CAS and 3D SiC/SiC post failure data show no change. The 2D SiC/SiC post-failure longitudinal velocity data appears to be degraded. One observes that when longitudinal fracture occurs cracks tend to close up and effectively restore pre-stress longitudinal modulus. This is the case for longitudinal velocity.

Response of SWF to Heat Treatment of the 3D SiC/SiC Composite

Two 3D SiC/SiC specimens were heat-treated at 1200 or 1550 °C in air for 100 hr and then SWF values were measured before tensile test. After tensile testing to failure at room temperature, SWF values were measured again. The results are shown in Fig. 13. A progressive degradation of centroid frequency occurs with higher heat-treatment temperature. The optical micrographs [10] showed that in fact there were more microstructural changes in specimens heat-treated at 1550 °C than specimens heat-treated at 1200 °C. SWF values after tensile tests reflected degradation due to mechanical loading only if compared within the same specimen. These results are consistent with those of Fig. 4.

CONCLUSIONS

Among the three AU parameters studied as a function of tensile failure, the stress-wave factor was to be the most consistent indicator of matrix crack formation for all three composite systems. The stress-wave factor was calculated as the centroid frequency of the AU waveform. The shift of the centroid to lower frequency is a manifestation of increased ultrasonic attenuation as internal damage progresses.

The advantage of centroid frequency over plate wave velocities is two fold. First, the centroid is directly dependent on attenuation caused by matrix cracking. The velocities are indirectly related through changes in stiffness caused by the cracking. Second, the centroid frequency calculation was less sensitive to fiber caused surface irregularity than were the plate wave pulses. Surface irregularity was sufficient to cause ambiguity in specimen thickness and plate wave boundary conditions. It may be of value for future applications to explore optimization of coupling conditions to rough surfaces for plate wave pulsing.

REFERENCES

1. Kautz, H.E.; and Bhatt, R.T.: Ultrasonic Velocity Technique for Monitoring Property Changes in Fiber-Reinforced Ceramic Matrix Composites. NASA TM-103806, 1991.
2. Vary, A.; and Bowles, K.J.: Use of Ultrasonic Acoustic Techniques for Nondestructive Evaluation of Fiber Composite Strength. Proceedings of 33rd Annual Conference, Sect. 24-A, SPI, NY, 1978, pp. 1-5.
3. Williams, J.H.; Yuce, H.; and Lee, S.S.: Ultrasonic and Mechanical Characterization of Fatigue States of Graphite Epoxy Composite Laminates, Mater. Eval., vol. 40, no. 5, 1982, pp. 560-565.
4. Kautz, H.E., Ultrasonic Evaluation of Mechanical Properties of Thick, Multilayered, Filament-Wound Composites, Mater. Eval., vol. 45, Dec. 1987, pp. 1404-1412.
5. Kautz, H.E.; and Lerch, B.A.: Preliminary Investigation of Acousto-Ultrasonic Evaluation of Metal-Matrix Composite Specimens. Mater. Eval., vol. 49, May 1991, pp. 607-612.

6. Vary, A.: Acousto-Ultrasonics. Non-Destructive Testing of Fibre-Reinforced Plastic Composites, Vol. 2, Ch. 1, Elsevier Science Publishing Co., New York, 1990, pp. 1-54.
7. Henneke, E.G., Jr.: Ultrasonic Nondestructive Evaluation of Advanced Composites, Non-Destructive Testing of Fibre-Reinforced Plastic Composites. Vol. 2, Ch. 2, Elsevier Science Publishing Co., New York, 1990, pp. 55-160.
8. Tang, B.; and Henneke II, E.G.: Long Wavelength Approximation for Lamb Wave Characterization of Composite Laminates. Res. Nondestr. Eval., vol. 1, no. 1, 1989, pp. 51-64.
9. Kautz, H.E.: Detecting Lamb Waves with Broad-Band Acousto-Ultrasonic Signals in Composite Structures. NASA TM-105557, 1992.
10. Chulya, A.; Gyekenyesi, J.Z.; and Gyekenyesi, J.P.: Failure Mechanisms of 3D Woven SiC/SiC Composites Under Tensile and Flexural Loading at Room and Elevated Temperatures. Ceram. Eng. Sci. Proc., vol. 13, July-Aug. 1992, pp. 420-432.
11. Tang, B.; and Henneke II, E.G.: Lamb-Wave Monitoring of Axial Stiffness Reduction of Laminated Composite Plates. Mater. Eval., vol. 47, Aug. 1989, pp. 928-934.
12. Weaver, R.L.: Diffuse Field Decay Rates For Material Characterization. Solid Mechanics Research for Quantitative Nondestructive Evaluation, J.D. Achenbach and Y. Rajapaskie, eds., Martinus Nijhoff Publishers, 1987, pp. 425-434.
13. Lott, L.A.; and Kunerth, D.C.: NDE of Fiber-Matrix Bonds and Material Damage in Ceramic/Ceramic Composites. Presented at the ASNT, Conference on Non-destructive Evaluation of Modern Ceramics, Columbus, OH, July 9-12, 1990.
14. Kautz, H.E., Determination of Plate Wave Velocities and Diffuse Field Decay Rates With Broad-Band Acousto-Ultrasonic Signals. To be presented at the ASNT Conference on Nondestructive Evaluation of Modern Ceramics, 1993.
15. Kiernan, M.T.; and Duke J.C., Jr.: A Physical Model for the Acousto-Ultrasonic Method. NASA CR-185294, 1990, p. 40.
16. Talreja, R.: Application of Acousto-Ultrasonics to Quality Control and Damage Assessment of Composites. Acousto-Ultrasonics: Theory and Application, J.C. Duke, Jr, ed., Plenum Press, New York, 1988, pp. 177-190.

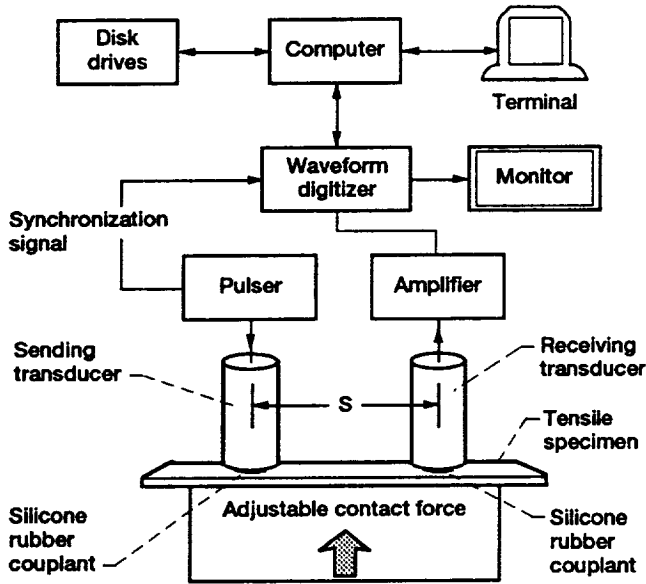


Figure 1.—Acousto-ultrasonic configuration employed for collecting data. The centerline spacing between the transducers, S is a variable in these experiments.

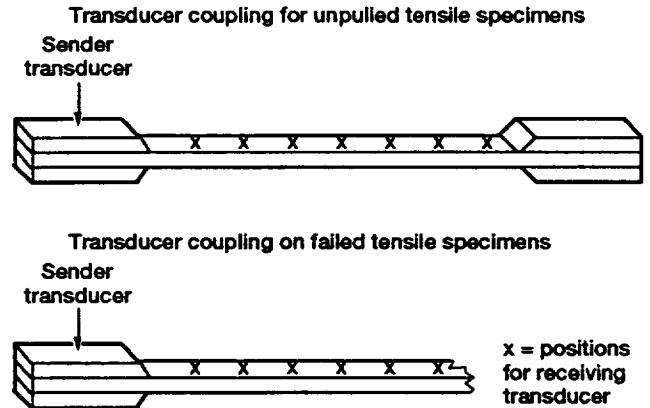


Figure 2.—Transducer coupling for platewave measurements.

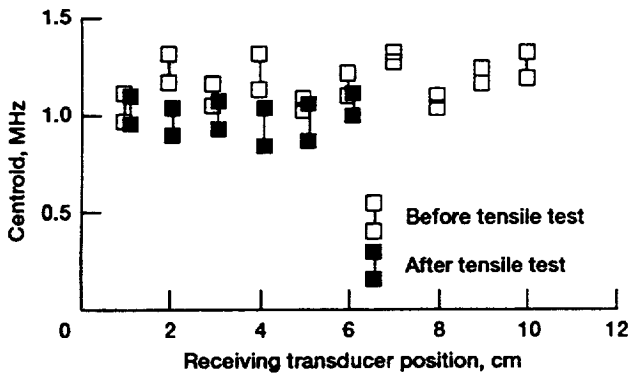


Figure 3.—Stress-wave factor data for two 3D SiC/SiC specimens. Tensile test was at elevated temperature. The specimen fracture is at the 6 cm location.

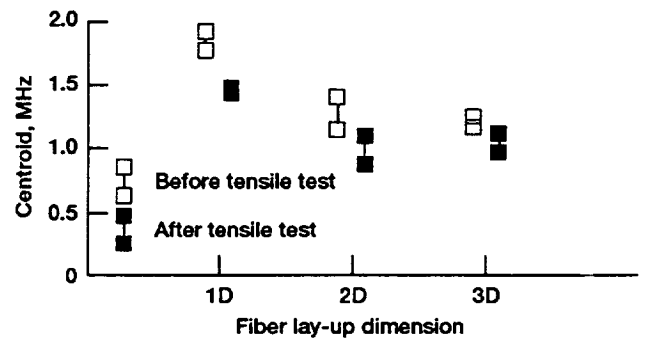


Figure 4.—Stress-wave factor data for three fiber architectures.

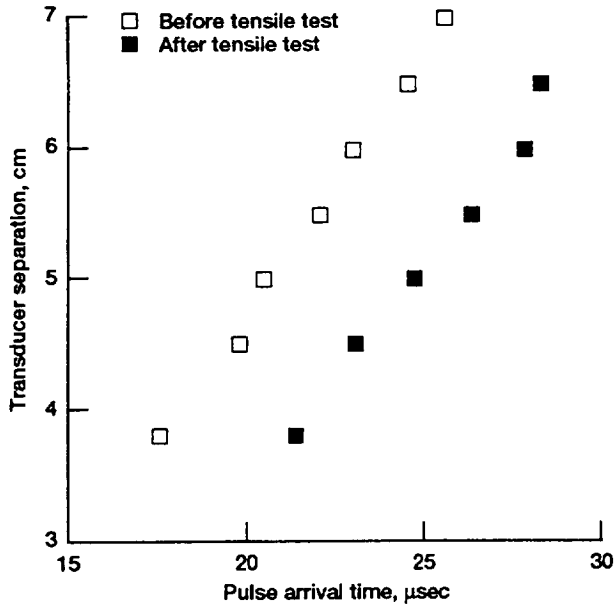


Figure 5.—First antisymmetric plate mode data from 1D SiC/CAS.

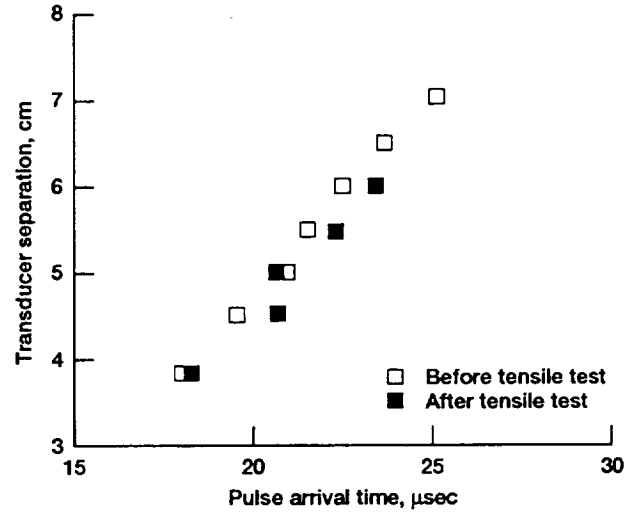


Figure 6.—First antisymmetric plate mode data from 2D SiC/SiC specimen.

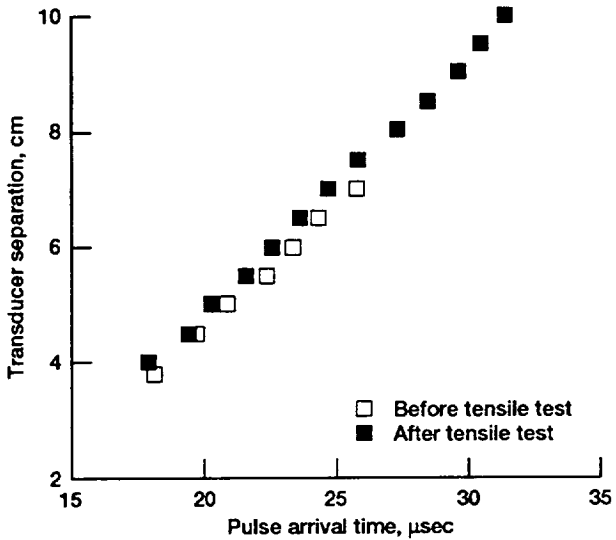


Figure 7.—First antisymmetric plate mode data from 3D SiC/SiC specimen failed at elevated temperatures.

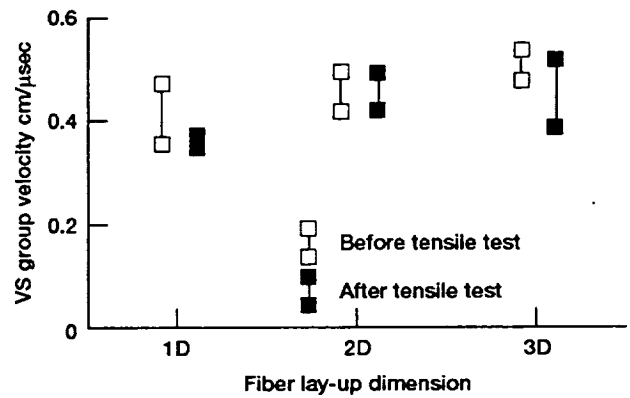


Figure 8.—First antisymmetric plate mode velocity for three fiber architectures.

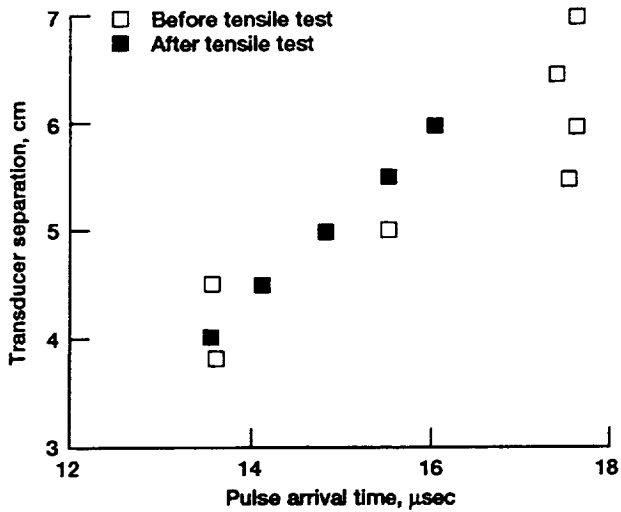


Figure 9.—First symmetric plate mode data from 1D SiC/CAS specimens.

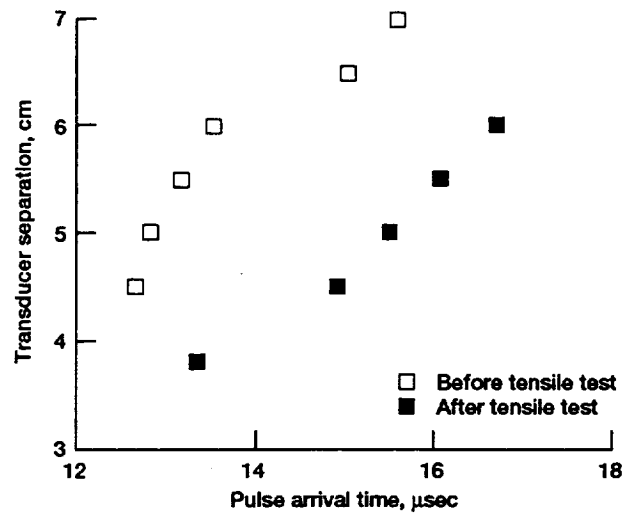


Figure 10.—First symmetric plate mode data from 2D SiC/SiC specimens.

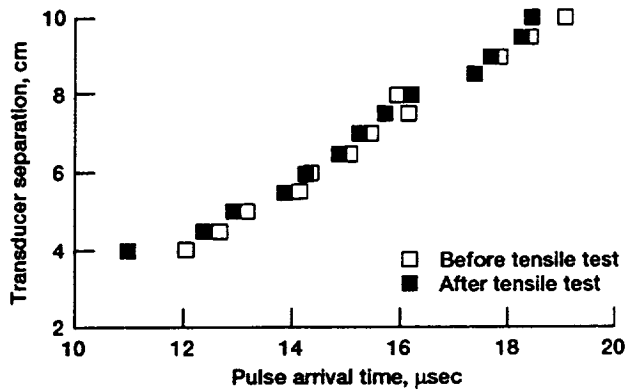


Figure 11.—First symmetric plate mode data from 3D SiC/SiC specimens failed at elevated temperatures.

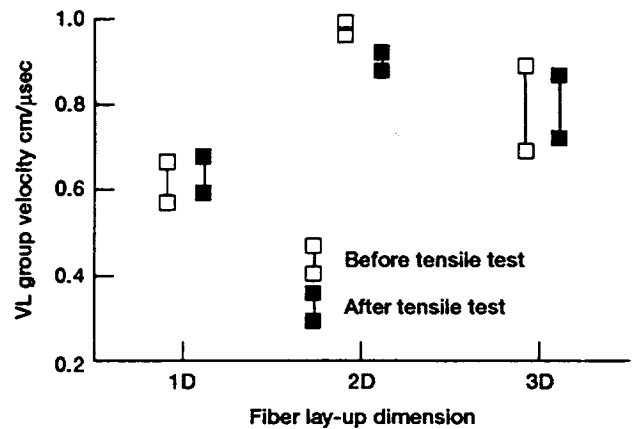


Figure 12.—First symmetric plate mode velocity for three fiber architectures.

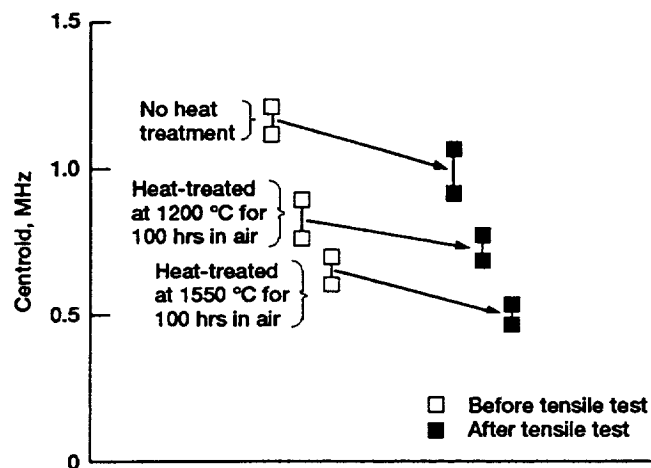


Figure 13.—Comparison stress-wave factor values in 3D SiC/SiC specimens that were heat-treated at 1200 and 1550 °C in air, as well as no heat-treatment, and then failed at room temperature.



REPORT DOCUMENTATION PAGE			Form Approved OMB No. 0704-0188	
Public reporting burden for this collection of information is estimated to average 1 hour per response, including the time for reviewing instructions, searching existing data sources, gathering and maintaining the data needed, and completing and reviewing the collection of information. Send comments regarding this burden estimate or any other aspect of this collection of information, including suggestions for reducing this burden, to Washington Headquarters Services, Directorate for Information Operations and Reports, 1215 Jefferson Davis Highway, Suite 1204, Arlington, VA 22202-4302, and to the Office of Management and Budget, Paperwork Reduction Project (0704-0188), Washington, DC 20503.				
1. AGENCY USE ONLY (Leave blank)	2. REPORT DATE June 1993	3. REPORT TYPE AND DATES COVERED Technical Memorandum		
4. TITLE AND SUBTITLE Acousto-Ultrasonic Analysis of Failure in Ceramic Matrix Composite Tensile Specimens			5. FUNDING NUMBERS WU-510-01-50	
6. AUTHOR(S) Harold E. Kautz and Abhisak Chulya				
7. PERFORMING ORGANIZATION NAME(S) AND ADDRESS(ES) National Aeronautics and Space Administration Lewis Research Center Cleveland, Ohio 44135-3191			8. PERFORMING ORGANIZATION REPORT NUMBER E-7930	
9. SPONSORING/MONITORING AGENCY NAME(S) AND ADDRESS(ES) National Aeronautics and Space Administration Washington, D.C. 20546-0001			10. SPONSORING/MONITORING AGENCY REPORT NUMBER NASA TM-106219	
11. SUPPLEMENTARY NOTES Prepared for the Second International Conference on Acousto-Ultrasonics sponsored by the American Society for Nondestructive Testing, Inc., Atlanta, Georgia, June 24-25, 1993. Harold E. Kautz, NASA Lewis Research Center, Cleveland, Ohio, and Abhisak Chulya, Cleveland State University, Cleveland, Ohio 44115. Responsible person, Harold E. Kautz, (216) 433-6015.				
12a. DISTRIBUTION/AVAILABILITY STATEMENT Unclassified - Unlimited Subject Category 38			12b. DISTRIBUTION CODE	
13. ABSTRACT (Maximum 200 words) Three types of acousto-ultrasonic (AU) measurements: stress-wave factor (SWF), lowest antisymmetric plate mode group velocity (VS), and lowest symmetric plate mode group velocity (VL), were performed on specimens before and after tensile failure. Three different Nicalon fiber architectures with ceramic matrices were tested. These composites were categorized as 1D (unidirectional fiber orientation) SiC/CAS glass ceramic, and 2D and 3D woven SiC/SiC ceramic matrix materials. SWF was found to be degraded after tensile failure in all three material categories. VS was found to be degraded only in the 1D SiC/CAS. VL was difficult to determine on the irregular specimen surfaces but appeared unchanged on all failed specimens. 3D woven specimens with heat-treatment at high temperature exhibited degradation only in SWF.				
14. SUBJECT TERMS Nondestructive testing; Ultrasonics; Ultrasonic testing ceramics; Ceramic matrix composites; Mechanical tests			15. NUMBER OF PAGES 10	
			16. PRICE CODE A02	
17. SECURITY CLASSIFICATION OF REPORT Unclassified	18. SECURITY CLASSIFICATION OF THIS PAGE Unclassified	19. SECURITY CLASSIFICATION OF ABSTRACT Unclassified	20. LIMITATION OF ABSTRACT	